

Effect of Heat Treatment and Electron Beam Irradiation Tourmaline: UV-Visible, EPR, and Mid-IR Spectroscopic Analyses**Apichate MANEEWONG^{*}, Kanwalee PANGZA,
Nongnuch JANGSAWANG and Tasanee CHAROENNAM***Gems Irradiation Center, Thailand Institute of Nuclear Technology (Public Organization),
Nakhon Nayok 26120, Thailand***(*Corresponding author's e-mail: mwchate@tint.or.th)***Presented at 41st Congress on Science and Technology of Thailand: November 6th - 8th 2015
Full paper accepted: 3 March 2016***Abstract**

The origin of the color change in 3 types of tourmaline gemstones, 2 pink samples from Afghanistan and one green sample from Nigeria, was examined by using UV-Vis, FTIR, EPR, and EDXRF spectroscopy. After heating at a temperature of 600 °C in air, the color of pink tourmaline gemstone changed to become colorless. This colorless tourmaline recovered its pink color by being irradiated with 800 kGy of electrons (e-beam). The UV-Vis absorption spectrum of the pink tourmaline with higher Mn concentration (T2, 0.24 wt%) showed characteristic absorption peaks originating from the Mn³⁺ color center: 2 absorption bands centered at wavelengths of 396 and 520 nm. Both absorption bands disappeared after heat treatment in air at 600 °C, and then displayed again after e-beam irradiation at 800 kGy. EPR spectra of T2 showed that the color change was related to the valence change of Mn³⁺ to Mn²⁺ ions and vice versa. The pink tourmaline of lower MnO content (T1, 0.08 wt%) also changed to being colorless with heat treatment, but the color was not recovered by e-beam irradiation. Instead, a yellow color was obtained. UV-Vis and FTIR spectra indicated that this yellow color originated from the decomposition of the hydroxyl group (-OH) into O⁻ and H⁰ by the e-beam irradiation. Green tourmaline did not show any color change with the heat treatment or the e-beam irradiation.

Keywords: Tourmaline, heat and electron treatment, UV-Vis, EPR, FTIR**Introduction**

Tourmaline is a group of chemically complex borosilicate minerals, and shows a variety of colors. The general formula can be expressed as XY₃Z₆(BO₃)₃(T₆O₁₈)V₃W, where X is a 9 coordination number (CN), which is occupied by Na⁺, Ca²⁺, K⁺, and a partial vacancy; the Y site 6 CN (octahedral polyhedron) is occupied by Mg²⁺, Fe²⁺, Mn²⁺, Al³⁺, Fe³⁺, Li⁺, Mn³⁺, and Cr³⁺; the Z site is 6 CN (octahedral), consisting mostly of Al³⁺, with minor impurities of Fe³⁺, Mg²⁺, Cr³⁺ and V³⁺; the T site is a tetrahedral site (4CN) occupied by Si⁴⁺, with small amounts of Al³⁺; the B site has 3 CN; the V site is OH⁻, and the W site is O²⁻ and F⁻ [1-3]. The optical properties of tourmaline are frequently governed by a cluster of transition metal cations located in the octahedral-Y sites, in which octahedra are face-shared with each other. The Y-octahedra cluster is connected to 3 smaller Z-octahedra along the edge. Both units serve as linkages along a 3-fold screw axis. The type, ordering, and distribution of cations occupying the Y and Z sites in the octahedral clusters also affect the crystal fields of the Mn and Fe ions.

Color and transparency are the most important aspects in evaluating the beauty and value of tourmaline. Heat treatment is most commonly used to alter its color, and is also used to increase its clarity. Heating can sometimes change overly dark pink stone to a lighter tone. Some previous studies have reported the effects of heat treatment. Heat treatment of blue tourmaline in air at 700 °C for 48 h of

can produce a red color due to the oxidation of ferrous iron at the octahedral site and simultaneous with the trap of the excess electron [4]. Recently, heat treatment was performed on schorl (black tourmaline) [5]. It was concluded that the black color changed to brown at 700 °C and reddish brown at 900 °C mainly due to oxidation of Fe. Although the thermal treatment effect has been reported in several studies, color enhancement was not achieved, due to the complexity of the tourmaline structure.

X-ray/gamma irradiation has long been one of the most popular methods used for enhancing the color of tourmaline. Many previous studies have clearly reported color changes by X-ray and gamma-ray exposure [6-10]. In contrast, the effect of e-beam irradiation has been pointed out only once in the literature [11]. The effect of electron beams on tourmaline has rarely been reported.

In this study, we investigated the color change of pink and green tourmaline, especially focusing on the color recovery mechanism shown by e-beam after heat treatment. The mineralogical study on all sample crystals was carried out with an energy dispersive X-ray fluorescence spectrometer (EDXRF), with UV-Vis spectroscopy, Electron paramagnetic resonance (EPR), and Fourier Transform Infrared Spectroscopy (FTIR). The combination of these techniques allowed the chemical characterization of the tourmaline samples to delineate the origin of the color and the color change along with the e-beam radiation and heat treatment.

Materials and methods

Two pink samples from Afghanistan and one green sample from Nigeria were prepared for investigation. Each sample was cut in half, perpendicular to the crystallographic *c*-axis. Subsequently, all samples were polished by silicon carbide abrasive paper. The evolution of the colors of the polished tourmaline samples with the heat treatment and e-beam irradiation was studied.

The Eagle-III μ Probe from EDAX, a new generation of X-ray micro-fluorescence (XRMF) spectrometer, was used for analyzing major oxides and trace elements contained in the 3 samples. The spectrometer was installed at the Department of Mineral Resources (DMR) under the Ministry of Natural Resources and Environment (MNRI) in Thailand, with a sample excitation by X-rays (Rh tube) focused by polycapillary fiber lens, minimum spot size 50 microns. An energy-dispersive liquid N₂-cooled Si detector with Be window was also used, suitable for detecting the XRF of chemical elements ranging from Na to U.

The polished natural gemstone samples were heated at 400 and 600 in air for 3 h. The heating rate of these holding temperatures was 100 °C/h. After heat treatment, the samples were cooled in the furnace.

The electron accelerator used in this study is located at the Gems Irradiation Center, Thailand Institute of Nuclear Technology (TINT), and can produce high energy, at 8 - 20 megavolt (MeV), and high power, at 10 kilowatt (kW). All our small samples were irradiated with 8 MeV of electron for 5 h to get an 800 kilogray (kGy) dosage. Due to the increase of the sample temperature induced by high power application on the stones during the electron beam processing, it was important to cool the stones. In our cases, water was used for the cooling process. The tourmaline samples were either placed in moving water or sprayed-water was used during the processing.

UV-Vis spectroscopic measurements on the platelets oriented parallel and perpendicular to the *c*-axis were measured before and after irradiation. UV-Vis spectroscopy measurement was performed using a PerkinElmer lambda 750 UV-Vis-NIR spectrophotometer at the Gems Irradiation Center, at the Ongkharak branch of TINT. UV-Vis spectra were recorded in the region of 200 - 800 nm at a scanning speed of 200 nm/min.

The tourmaline samples prepared for the EPR studies were ground into fine powder in a mortar. All EPR measurements were performed at room temperature on a Bruker EPR spectrometer (ESP 300 series) operated in the X-band microwave frequency at the Seoul branch of the Korea Basic Science Institute. The spectrometer operating conditions adopted during the experiment were: 350.0 mT central magnetic field; 140 - 600 mT scan ranges; 9.64 GHz microwave frequency; 1.0 mW microwave power; 100 kHz field modulation frequency; 1.0 mT field modulation amplitude, and 0.02 s time constant.

Mid-infrared spectra of tourmaline samples were recorded in the whole range from 400 to 5000 cm^{-1} using a Bruker ALPHA Spectrometer with 100 scans and 4 cm^{-1} resolution at DMR. Band fittings were done using the fitting program Origin 8.0 with the Gauss-Lorentz function.

Results and discussion

The chemical compositions of 3 tourmaline samples are shown in **Table 1**. EDXRF analysis indicated that all the tourmalines were fluor-elbaite, with fluorine weight fractions 2.59, 2.68, and 1.98 %, named T1, T2 and T3, respectively. They also contained significant amounts of MgO and MnO. While a small quantity of FeO was found in T1 and T2, the T3 sample (green) had a large amount of FeO, 5.70 %. Cr_2O_3 and ZnO existed at an impurity level. The T2 pink tourmaline had higher amounts of MnO than the T1 pink tourmaline. T3 contained much high amounts of MnO and FeO.

Table 1 Chemical composition of 3 tourmaline samples by EDXRF analysis.

Sample no.	T1 (Pink)	T2 (Pink)	T3 (Green)
<i>Oxide: (wt%)</i>			
SiO ₂	37.20	36.87	34.61
Al ₂ O ₃	42.10	41.26	36.73
MgO	2.19	2.23	2.05
Na ₂ O	0.48	0.75	0.71
K ₂ O	0.04	0.03	0.04
CaO	0.08	0.18	1.47
TiO ₂	0.01	0.01	0.09
Cr ₂ O ₃	0.01	0.01	Nd
MnO	0.08	0.24	2.59
ZnO	Nd	Nd	0.55
FeO	0.02	0.03	5.70
F	2.59	2.68	1.98
B ₂ O ₃ *	11.01	10.91	10.71
Li ₂ O*	1.20	1.26	1.11
H ₂ O*	2.57	2.50	2.75
Subtotal	99.36	98.95	101.09
O=F	1.09	1.13	0.83
Total	98.27	97.82	100.26

*B₂O₃, Li₂O and H₂O calculated by stoichiometry
 Nd = not detected

The results of the heat treatments regarding color change of the samples are summarized in **Table 2**. At 400 °C, all 3 samples showed almost no change. After heating at 600 °C, the 2 pink samples showed an obvious change in becoming colorless. However, the green sample remained the same color as before the heat treatment.

Table 3 shows the effect of e-beam irradiation on the color of the 3 samples which were heat treated at 600 °C. When irradiated with electrons at 400 kGy, the 2 colorless tourmalines partially recovered their pink color. T1 displayed a pink-yellow color, whereas T2 became pink, which is close to the natural state. T3 did not show any color change. Upon increasing the e-beam dosage to 600 kGy, the pink-yellow color in T1 changed to yellow. On the other hand, T2 completely recovered its original pink color. Again, T3 still showed no changes in color.

The UV-Vis absorption spectra (E_{1c}) of the 2 pink tourmalines (T1 and T2) are represented in **Figures 1a** and **1b**, respectively. Both natural pink tourmalines showed broad absorption bands at 396

and 520. After heating at 400 °C, the absorption bands at 396 and 520 of both pink tourmalines had decreased in their intensity (represented by a dash line). When heated at 600 °C, these peaks had disappeared (represented by a square symbol line), which conforms to the disappearance of color in both samples.

Table 2 Heat treatment results for the 3 samples.

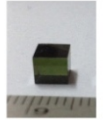
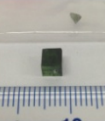
Heating temperature	T1	T2	T3
0 °C (natural)	 Pale pink	 Pale pink	 Dark green
400 °C	 Slightly lighter	 Slightly lighter	 No change
600 °C	 Colorless	 Colorless	 No change

Table 3 E-beam irradiation results for the samples.

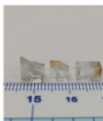
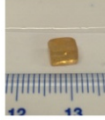
Absorbed dose	T1	T2	T3
0 kGy (after heating 600 °C for 3 h)	 Colorless	 Colorless	 Dark green
600 kGy	 Pink-yellow	 Pale pink	 No change
800 kGy	 Yellow	 Deep pink	 No change

Figure 1a also shows the absorption spectra of T1 after e-beam irradiation, which appears as a yellow color. With an electron dose 600 kGy, a small broad absorption band at 520 nm reappeared (represented by a circle symbol line). In particular, the based-line of the absorption spectra over the range of 300 ~ 550 nm steeply increases with e-beam irradiation. With increasing e-beam dosage to 800 kGy, the base-line appears the same as that of the 600 kGy sample. It appears that the 2 absorption peaks at 396 and 520 were substituted by an increase of the background over the range of 300 ~ 550 nm. The yellow color of the e-beam irradiated T1 can be ascribed to the drastic increase of the background line of the absorption spectrum over the 300 ~ 550 nm. These absorption peaks existed in the e-beam irradiated samples (represented by triangle and open circle symbols).

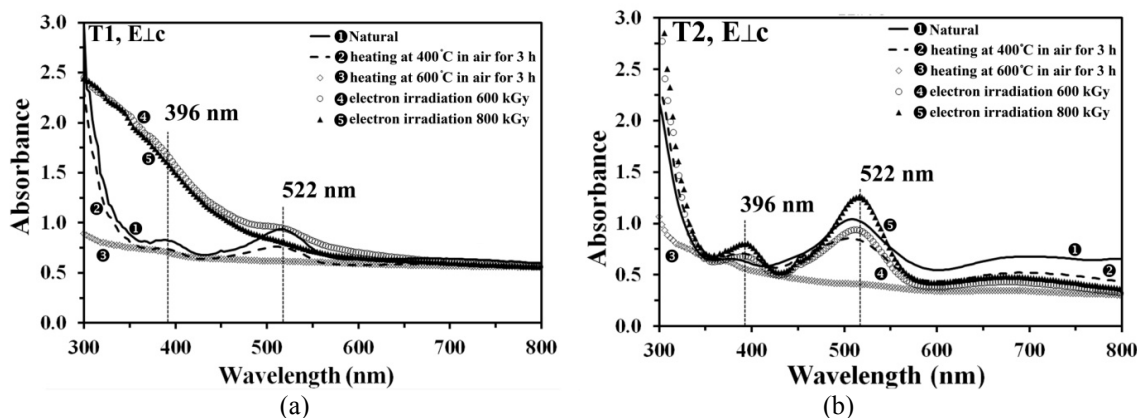


Figure 1 UV-Vis spectra of 2 pink tourmalines: T1 (a) and T2 (b) sample.

The recovery of pink color by e-beam irradiation of the colorless T2 (after heating) can be confirmed by the absorption spectrum shown in **Figure 1b**. After heat treatment, the 2 absorption bands at both at 396 and 520 nm disappeared. However, by using irradiating e-beam (600 kGy), these 2 absorption peaks reappeared, and the intensity of both peaks increased when raising the dosage to 800 kGy (represented by a triangle symbol line).

Several interpretations for the 2 bands at 396 and 520 nm have been suggested. Both absorption bands can come from Mn^{3+} and/or $Mn^{2+} - Mn^{3+}$ [8,12,13]. At first, these absorption bands in natural pink samples cannot originate from Mn^{2+} , because the d-d electronic transition of Mn^{2+} (d^5 configuration) is spin-forbidden and hence has very low absorption coefficients [14]. On the other hand, Mn^{3+} (d^4 configuration) has a strong absorption coefficient, because its electronic transition is permitted and the crystal field is very asymmetric due to the compressed octahedron in the Y site along the OH_1-OH_3 axis [11].

After heating at 400 °C for 3 h in air, the pink samples became a slightly lighter pink, and became colorless when increasing the temperature to 600 °C. These results can be ascribed to the reduction of Mn^{3+} to Mn^{2+} by heat treatment.

With electron irradiation at 600 kGy, T1 displayed a pink-yellow color, and then changed to yellow when increasing the electron dose to 800 kGy. This color change to yellow, both at 600 and 800 kGy, can be ascribed to the substantial increase of the back ground in the absorption spectra (300 ~ 550 nm range, **Figure 1**). This absorption background (300 ~ 550 nm range) has been suggested by Krambrock *et al.* [2]. It was suggested to be located at the O^- hole trap center in the OH site. If tourmaline is irradiated by an electron beam, the OH^- molecule in the OH site will be decomposed into O^- (hole trap) and H^0 (electron trap). In contrast, T2 recovered its deep pink color by e-beam irradiation at an 800 kGy dosage. In T2, the background of the absorption spectra remained the same as before e-beam irradiation. This indicates that the OH group did not decompose by e-beam irradiation, which may due to the percentage of water in T2

being lower than in T1. The 2 strong absorption bands at 390 and 520 nm in T2 reappeared by the irradiation, which indicates that the Mn^{2+} ions oxidized to Mn^{3+} .

Figure 2 shows the absorption spectra ($E_{\perp c}$) of green tourmaline (T3). After heat treatment the absorption maxima in the vicinity of 700 nm slightly decreased. The intensity of this broad absorption band decreases further by the e-beam dosage of 800 kGy. Even with the slight decrease, the intensity of the color remained the same.

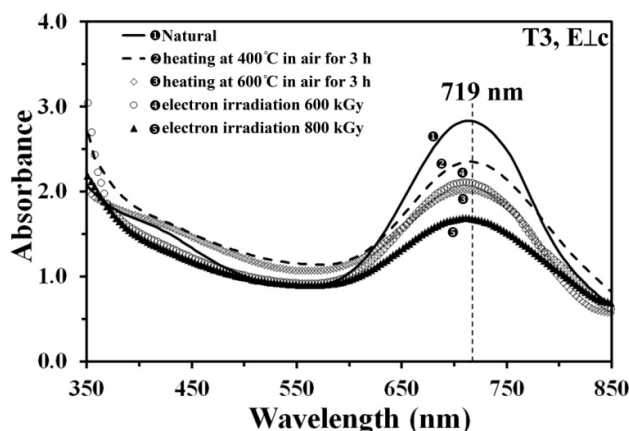


Figure 2 UV-Vis spectra of T3 sample.

The absorption maximum in the vicinity of 700 nm in green tourmaline has been reported in several previous works [15-18]. This band occurred due to presence of Fe^{2+} or Cu^{2+} , which originated a greenish blue color. Since there were no Cu ions (**Table 1**) in T3, one possible reason for the intensity decrease of the absorption band (~ 700 nm) can be ascribed to the exchange interaction $Fe^{2+} \leftrightarrow Fe^{3+}$, as suggested by previous work [11]. It appears that partial oxidation of Fe^{2+} occurred during heat treatment in air, in which oxidation could decrease the intensity of the absorption band at 700 nm. After subsequent e-beam irradiation, the intensity of this band slightly increased. However, the oxidation/reduction reactions produced by these treatments were not enough to change the color of T3. Using other atmosphere, i.e., nitrogen gas heated, and diffusion treatment, may more suitable, as suggested by Castaneda *et al.* [4].

EPR was used in this study for investigating the chemical status of paramagnetic ions Fe^{3+} , Mn^{2+} , and their valence change upon heating and electron irradiation. The X-band EPR spectra of T1 and T2 are shown in **Figures 3a** and **3b**, respectively.

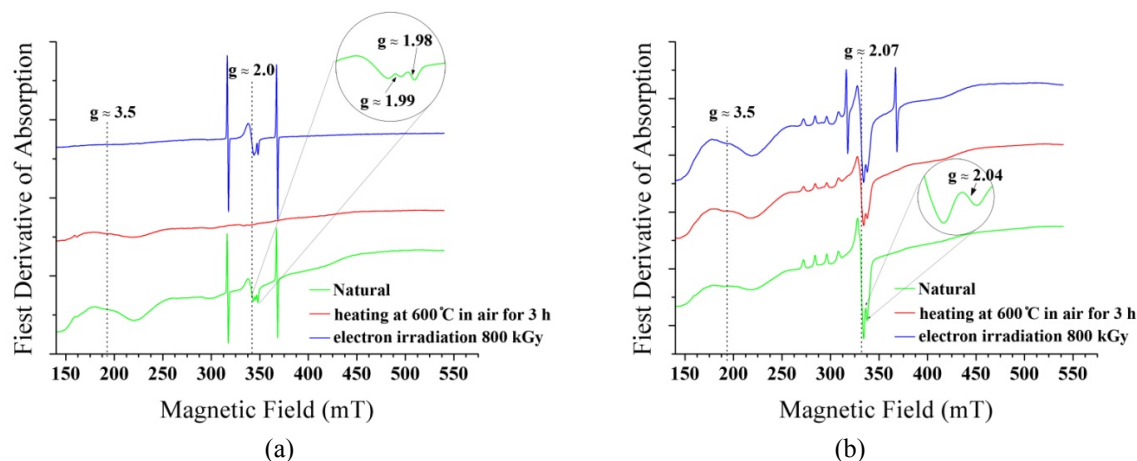


Figure 3 EPR Spectra of T1 (a) and T2 (b).

All investigated samples exhibited resonance signals. The natural state of T1 (represented by a green line in **Figure 3a**) showed a relatively sharp signal at $g \approx 2.0$ (with line width $\Delta B_{pp} = 4 - 5$ mT) and a very broad peak at $g \approx 3.5$ ($\Delta B_{pp} = 35 - 40$ mT). The resonance signal of the standard sample used in the process of calibration appeared at $g \approx 1.87$ and 2.17 . The green line (natural T2) in **Figure 3b** showed a relatively sharp signal ($\Delta B_{pp} = 4 - 5$ mT) at $g \approx 2.07$ and a broad peak at $g \approx 3.5$ ($\Delta B_{pp} = 35 - 40$ mT), including the 6 hyperfine lines around $g \geq 2.07$. The EPR spectra of T3 were different from T1 and T2. Due to the high concentration of Mn (2.59 %wt) and Fe (5.70 %wt), broad resonance signals appeared.

Several previous literatures on EPR spectra of Mn^{2+} in various materials observed resonance signals at $g \approx 2.0$, $g \approx 2.5$, $g \approx 3.5$, $g \approx 4.3$, and the 6th line hyperfine [19,20]. Fe^{3+} also showed resonance signals at $g \approx 2.0$, $g \approx 4.3$, $g \approx 6.0$, and $g \approx 10.0$ [21]. Recent EPR studies on tourmaline (Fe-poor elbaite) assigned signals at $g \approx 2.5$ and 3.5 to Mn^{2+} and signals at $g \approx 4.3$ and 2.0 to Fe^{3+} [22]. The EPR spectra of T1 and T2 natural state (represented by a green line in **Figures 3a** and **3b**) indicated that the signals at $g \approx 2.0$ and 3.5 corresponded to Mn^{2+} and/or Fe^{3+} . The signal at $g \approx 2.0$ (T1, T2) can be attributed to isolated Mn^{2+} and/or Fe^{3+} ions in a strongly distorted octahedral surrounding. The broad signal at $g \approx 3.5$ can be related to magnetically coupled clusters of Mn^{2+} -O- Mn^{3+} or Mn^{2+} -O- Fe^{3+} [23]. The Fe^{3+} affects the observed EPR signals lesser degree than Mn^{2+} due to low content of Fe in both pink samples (see **Table 1**). The insets (see **Figure 3**) showed additional small signals at $g \approx 2.0$. These small signals might have come from Fe^{3+} . In T1, the resonance signals at $g \approx 2.0$, and $g \approx 3.5$ showed significantly lower intensity after heating at 600 °C. This decrease might have occurred due to microheterogeneous regions of Mn^{2+}/Mn^{3+} or Mn^{2+}/Fe^{3+} clusters, which diffuse out by heat treatment. After being irradiated with 800 kGy, the resonance signal at $g \approx 2.0$ reappeared. This signal could be ascribed to the partial reduction of isolated Mn^{3+} to Mn^{2+} and/or Fe^{2+} to Fe^{3+} by e-beam. Hence, we could tentatively ascribe the pink color of T1 to the Mn and/or Fe ions related to $g \approx 2.0$ signals. The oxidation/reduction behavior of Mn ions by the thermal/electronic treatments in T1 is rather ambiguous compared to T2.

T2 showed a rather different EPR behavior to T1. After heating at 600 °C, the signal at $g \approx 2.07$ significantly decreased, whilst the signal at $g \approx 3.5$ slightly increased. This indicated that magnetic coupling of Mn^{2+} -O- Mn^{3+} or Mn^{2+} -O- Fe^{3+} clusters slightly increased at a partial expense of the isolated Mn^{2+} ions ($g \approx 2.07$). The intensity of the 6 hyperfine lines also decreased by heating at 600 °C. This indicated that the absorption bands at 390 and 520 nm in T2 could have originated from the isolated Mn and/or Fe^{3+} ions related to the resonance signal at $g \approx 2.07$. After being irradiated with electrons at 800 kGy, the intensities of both signals at $g \approx 2.07$ and $g \approx 3.5$ increased. Therefore, the pink color in T2 also

can be ascribed to the isolated Mn and/or Fe ions giving rise to the resonance at $g \approx 2.07$. In addition, the intensity of the 6 hyperfine lines also slightly increased after the irradiation of 800 kGy.

The mid-infrared spectrum of tourmalines is very sensitive to transition metal variations [24]. In the OH⁻ stretching region, it is easy to distinguish the inner hydroxyl group, with low-intensity bands at high wavenumbers, from the 3 outer ones which produce broad high-intensity low-wavenumber bands. The high-wavenumber bands ($> 3600 \text{ cm}^{-1}$) are particularly sensitive to the X-site occupancy (Na or □), and to the cation distribution over the adjacent Y sites (Mn²⁺, Mn³⁺). The lower wavenumber bands (3600 - 3300 cm^{-1}), reveal the cationic distribution over the Y and Z sites with great accuracy. Furthermore, the combination stretching and bending modes of the cationic hydroxyl units were observed in the region of 4800 - 4400 cm^{-1} . Our analyzed spectra were shown to be rather similar to these mentioned spectra.

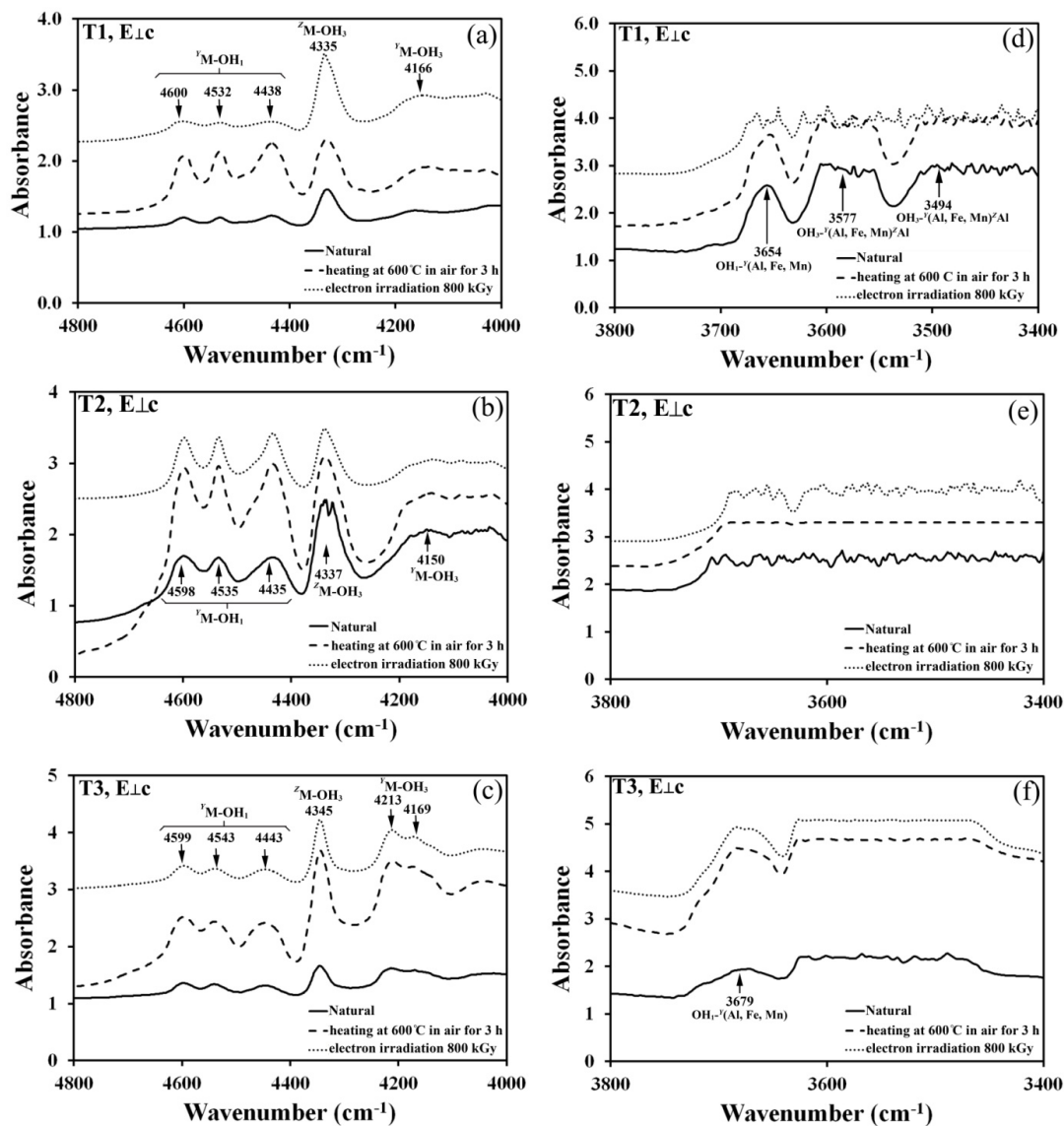


Figure 4 Mid-infrared spectra in 4800 - 4000 cm^{-1} region for T1 (a), T2 (b), and T3 (c), and 3800 - 3400 cm^{-1} region for T1 (d), T2 (e), and T3 (f).

The spectra of all 3 samples in natural state were shown to be rather similar. T3 had the highest intensity peaks at 4345 cm^{-1} , following by T2 and T1. The weak bands appeared in the range $2800 - 2500\text{ cm}^{-1}$ and the strong intensity bands from 3000 to 3750 cm^{-1} . The moderately intense bands appeared at around $4800 - 4400\text{ cm}^{-1}$. These bands in this range were assigned to the combination of the stretching and bending modes of cationic hydroxyl units (MOH where M is Al, Mg, Fe, Mn, etc.) by Reddy [3].

The absorption band (E_{1c}) of samples T1, T2, and T3 in the $4800 - 4000\text{ cm}^{-1}$ region before and after treatment are shown in **Figures 4a, 4b and 4c**, respectively. All samples exhibited similar behavior by showing absorption bands near $4600, 4530, 4440, 4340$, and between $4300 - 4100\text{ cm}^{-1}$. The combination of the stretching and bending modes of ${}^Y\text{M-OH}_1$ commonly led to the bands at $4600, 4530, 4440\text{ cm}^{-1}$. Changes in absorption band intensity at each step of treatment indicated that the combination bands of ${}^Y\text{M-OH}_1$ units were slightly affected by ${}^Y\text{M}$ metallic ions due to the hydroxyl groups at *W* site. The intensity increase of these bands after heating indicated that the bond distances between the metal ions and the hydroxyl group had changed. All samples showed increases in intensity at the bands $4600, 4530$, and 4440 cm^{-1} after heating at $600\text{ }^\circ\text{C}$. The intensity decreased by subsequently being irradiated with 800 kGy . The absorption bands at 4600 cm^{-1} were suggested to be combination bands involving Al-OH units [3]. Therefore, the absorption bands near 4600 cm^{-1} were considered to be combination bands involving ${}^Y\text{Al-OH}_1$. The observed combination band near 4340 cm^{-1} occurred due to the combination of the stretching and bending modes of ${}^Z\text{M-OH}_3$ [25]. The *Z* sites in the 3 elbaite samples were mainly occupied by Al^{3+} . Therefore, ${}^Z\text{M-OH}_3$ units were mainly composed of ${}^Z\text{Al-OH}_3$. Similar with those bands, the intensity of the band near 4340 cm^{-1} increased after heating and decreased after being subsequently irradiated with electrons. The 2 bands in the range of $4300 - 4100\text{ cm}^{-1}$ were considered to be a combination of the stretching and bending modes of ${}^Y\text{M-OH}_3$, in which the units were much more complex, with many types of metallic ions located at the *Y* site.

T1 showed the most drastic decrease in intensity of the bands at $4600, 4530, 4440$ and 4340 cm^{-1} after being irradiated with electrons at 800 kGy . This intensity decrease indicated the decomposing of OH⁻ group into O⁻ (hole trap) and H⁰ (electron trap), resulting in the decrease in intensity. However, the decomposition phenomenon was less severe in T2 and T3. Hence, only T1 changed to yellow by e-beam irradiation. In T1, after heating and being subsequently irradiated with electron, electron- hole trap (color centers) was the main cause of color, while the existence of Mn^{2+} and Mn^{3+} in T2 caused the pink color.

Figures 4d, 4e and 4f show the spectra in the range of $3850 - 3350\text{ cm}^{-1}$ of the 3 samples. These bands were considered as the hydroxyl stretching modes [3,8,26]. The absorption bands at 3490 and 3578 cm^{-1} were assigned for the stretching modes of the $-\text{OH}_3$ groups, whereas the band at 3671 cm^{-1} was attributed to the stretching modes of the $-\text{OH}_1$ groups. Those 3 absorption bands were clearly visible in T1, whereas they do not appear in T2, and T3 shows only one absorption band at around 3680 cm^{-1} . The intensity change of these absorption bands after treatment was related to the distance between the metal ions and the hydroxyl group.

Conclusions

Pink tourmalines became colorless after heating at $600\text{ }^\circ\text{C}$. The pink tourmaline with higher manganese content could recover its pink color by electron irradiation. This is ascribed to the partial oxidation/reduction reaction of isolated Mn ions simultaneously with Fe ions. The EPR spectra indicated there were 2 types of environments for Mn ions: isolated and clustered states. Mid-infrared spectra in the ranges of $3800 - 3400\text{ cm}^{-1}$ and $4800 - 4000\text{ cm}^{-1}$ were related to hydroxyl stretching modes. Heat treatment and electron irradiation affected the stretching modes of ${}^Y\text{M}$ metallic ions. T1 showed the most drastic decrease in intensity of the bands, at $4600, 4530, 4440$, and 4340 cm^{-1} after being irradiated with electrons at 800 kGy . The decomposing of the OH⁻ group into O⁻ (hole trap) and H⁰ (electron trap) resulted in a decrease in intensity. This decomposition resulted in the yellow color in T1. The decomposition phenomenon was less severe in T2 and T3. Hence, only T1 was changed to yellow by e-beam irradiation. Heating and electron irradiation did not affect the color of green tourmaline. Heat treatment and electron irradiation can be effective methods for the color enhancement of pink tourmaline. The color change may occur through different mechanisms, depending on, most of all, the composition of

tourmaline. Then, it depends on the conditions, such as the temperature and the time of the heat treatment, the dose and the type of irradiation, the procedure of irradiation and the heat treatment, and the quantity of impurities present in the mineral.

References

- [1] C Castaneda, EF Oliveira, N Gomes and ACP Soares. Infrared study of OH sites in tourmaline from the elbaite-schorl series. *Am. Mineral.* 2000; **85**, 1503-7.
- [2] K Krambrock, MVB Pinheiro, SM Medeiros, KJ Guedes, S Schweizer and JM Spaeth. Investigation of radiation-induced yellow color in tourmaline by magnetic resonance. *Nucl. Instrum. Meth. B* 2002; **191**, 241-5.
- [3] BJ Reddy, RL Frost, WN Martens, DL Wain and JT Kloprogge. Spectroscopic characterization of Mn-rich tourmalines. *Vib. Spectros.* 2007; **44**, 42-9.
- [4] C Castaneda, SG Eeckhout, GMD Costa, NF Botelho and ED Grave. Effect of heat treatment on tourmaline from Brazil. *Phys. Chem. Mineral.* 2006; **33**, 207-16.
- [5] P Bačík, D Ozdín, M Miglierini, P Kardošová, M Pentrák and J Haloda. Crystallochemical effects of heat treatment on Fe-dominant tourmalines from Dolní Bory (Czech Republic) and Vlachovo (Slovakia). *Phys. Chem. Mineral.* 2011; **38**, 599-611.
- [6] GH Faye, PG Manning, JR Gosselin and RJ Tremblay. The optical absorption spectra of tourmaline: Importance of charge-transfer processes. *Can. Mineral.* 1974; **12**, 370-80.
- [7] MBD Camargo and S Isotani. Optical absorption spectroscopy of natural and irradiated pink tourmaline. *Am. Mineral.* 1988; **73**, 172-80.
- [8] IM Reinitz and GR Rossman. Role of natural radiation in tourmaline colouration. *Am. Mineral.* 1988; **73**, 822-5.
- [9] I Petrov. Role of natural radiation in tourmaline coloration: Discussion. *Am. Mineral.* 1990; **75**, 237-9.
- [10] BM Laurs, JC Zwaan, CM Breeding, WB Simmons, D Beaton, KF Rijdsdijk, R Befe and AU Falster. Copper-bearing (Paraíba-type) tourmaline from Mozambique. *Gem. Gemol.* 2008; **44**, 4-30.
- [11] YK Ahn, JG Seo and JW Park. Electronic and vibrational spectra of tourmaline - The impact of electron beam irradiation and heat treatment. *Vib. Spectros.* 2013; **65**, 165-75.
- [12] PG Manning. Effect of second-nearest-neighbor interaction on Mn³⁺ absorption in pink and black tourmalines. *Can. Mineral.* 1973; **11**, 971-7.
- [13] GR Rossman and SM Mattson. Yellow Mn-rich elbaite with Mn-Ti intervalence charge transfer. *Am. Mineral.* 1986; **71**, 599-602.
- [14] DM Sherman and N Vergo. Optical spectrum, site occupancy and oxidation state of Mn in montmorillonite. *Am. Mineral.* 1988; **73**, 140-4.
- [15] GH Faye, PG Manning and EH Nickel. The polarized optical absorption spectra of tourmaline, cordierite, chloritoid and vivianite: Ferrous-ferric electronic interaction as a source of pleochroism. *Am. Mineral.* 1968; **53**, 1174-201.
- [16] SM Mattson and GR Rossman. Fe²⁺-Fe³⁺ interactions in tourmaline. *Phys. Chem. Mineral.* 1987; **14**, 163-71.
- [17] GR Rossman, E Fritsch and JE Shigley. Origin of color in cuprian elbaite from São José de Batalha, Paraíba, Brazil. *Am. Mineral.* 1991; **76**, 1479-84.
- [18] G Smith. Evidence for absorption by exchange-coupled Fe²⁺-Fe³⁺ pairs in the near infra-red spectra of minerals. *Phys. Chem. Mineral.* 1978; **3**, 375-83.
- [19] N Srisittipokakun, C Kedkaew, J Kaewkhao, T Kittiauchawal, K Thamaphat and P Limsuwan. Electron spin resonance (ESR) and optical absorption spectra of a manganese doped soda-lime-silicate glass system. *Kasetsart J. Nat. Sci.* 2009; **43**, 360-4.
- [20] RPS Chakradhar, G Sivaramaiah, JL Rao and NO Gopal. EPR and optical investigations of manganese ions in alkali lead tetraborate glasses. *Spectrochim Acta A* 2005; **62**, 761-8.

- [21] RS Muralidharaa, CR Kesavulub, JL Raob, RV Anavekara and RPS Chakradharc. EPR and optical absorption studies of Fe³⁺ ions in sodium borophosphate glasses. *J. Phys. Chem. Solids* 2010; **71**, 1651-5.
- [22] J Babińska, K Dyrek, A Pieczka and Z Sojka. X and Q band EPR studies of paramagnetic centres in natural and heated tourmaline. *Eur. J. Mineral.* 2008; **20**, 233-40.
- [23] SP Chaudhuri and SK Patra. Electron paramagnetic resonance and Mössbauer spectroscopy of transition metal ion doped mullite. *J. Mater. Sci.* 2000; **35**, 4735-41.
- [24] T Gonzalez-Carrefio and M Fernandez. Infrared and electron microprobe analysis of tourmalines. *J. Sanz. Phys. Chem. Mineral.* 1988; **15**, 452-60.
- [25] X Liu, X Feng, J Fan and S Guo. Optical absorption spectra of tourmaline crystals from Altay, China. *Chin. Opt. Lett.* 2011; **9**, 083001.
- [26] D Cao, G Zhao, Q Dong, J Chen, Y Cheng, Y Ding and J Zou. Effects of annealing on luminescence efficiency of large-size YAG: Ce crystal grown by temperature gradient techniques. *Chin. Opt. Lett.* 2010; **8**, 199-201.